

Optical spin orientation of an individual Mn^{2+} ion in a CdSe/ZnSe quantum dot

T. Smoleński,* W. Pacuski, M. Goryca, M. Nawrocki, A. Golnik, and P. Kossacki

Institute of Experimental Physics, Faculty of Physics, University of Warsaw, Hoża 69, 00-681 Warsaw, Poland

(Received 21 August 2014; revised manuscript received 18 December 2014; published 30 January 2015)

We demonstrate optical spin orientation of an individual Mn^{2+} ion embedded in a CdSe/ZnSe quantum dot. It is achieved through the injection of spin-polarized excitons to the dot under circularly polarized below-the-barrier optical excitation at energy sufficiently close to the dot emission energy. The efficiencies of both the exciton spin-transfer and optical pumping of the Mn^{2+} spin are studied by means of polarization-resolved single-dot spectroscopy performed at magnetic field in a Faraday configuration. The ion spin orientation efficiency is found to increase significantly with the magnetic field, while the spin-polarization degree of injected excitons remains constant and yields about 40%.

DOI: [10.1103/PhysRevB.91.045306](https://doi.org/10.1103/PhysRevB.91.045306)

PACS number(s): 78.67.Hc, 78.55.Et, 75.75.-c

I. INTRODUCTION

Studies of single objects in solids have recently attracted a lot of research attention. This led to coining the term *solotronics* — optoelectronics based on solitary dopants [1–4]. To achieve the control over a single dopant, in particular over its spin, different techniques were employed depending on the studied system. For example, electrical control of a single phosphorus center on the Si surface allowed to realize a single atom transistor [5] and qubit [6,7]. The second approach relied on resonant driving of an internal optical transition of a defect, which was demonstrated for nitrogen-vacancy (N-V) centers in diamond [8] and lanthanide ions [9–11].

Transition metal ions with a partially filled d shell embedded in a semiconductor offer another attractive possibility of optical manipulation mediated by spin-polarized carriers, which interact with the magnetic ion due to the $s, p-d$ exchange interaction [12]. Such an interaction leads to particularly interesting effects when an individual magnetic ion is embedded in a quantum dot (QD) [13]. In such a case, the excitonic states are split due to the interaction with the individual magnetic ion, allowing an unambiguous readout of the magnetic-ion spin state from the polarization and energy of the photon emitted from such a system.

So far four systems of QDs with single magnetic dopants have been reported: the individual manganese ion in a CdTe [13], InAs [14], and CdSe QD [4], and the individual cobalt ion in a CdTe QD [4]. The optical manipulation of the ion spin has been demonstrated only in the case of CdTe and InAs QDs containing manganese ions. It has been achieved either by strictly resonant excitation of exchange-split excitonic states [15–17] or through injection of spin-polarized excitons to a Mn-doped QD [18–20]. Such an injection typically requires efficient spin-conserving excitation channels. They have been found for CdTe/ZnTe QDs with the use of resonant excitation of either an excited excitonic state in Mn-doped QD [18], or a ground state of the neutral exciton in an adjacent, spontaneously coupled nonmagnetic dot [19–22]. However, the possibility of such resonant excitation has not been demonstrated for a CdSe/ZnSe QD containing a single Mn^{2+} ion — a new promising solotronic system with very long

Mn^{2+} spin relaxation time [4,23,24]. Instead, self-organized CdSe/ZnSe QDs offer a possibility to employ nonresonant, but still spin-conserving optical excitation channels, as was shown for QD ensembles [25]. In this work we demonstrate that such a channel can be exploited to optically orient the spin of a single Mn^{2+} ion embedded in a CdSe/ZnSe QD.

II. SPECTROSCOPY OF CDSE/ZNSE QDS WITH SINGLE Mn^{2+} IONS

The sample studied in this work contains a single layer of self-assembled CdSe/ZnSe QDs doped with Mn^{2+} ions. It is grown using molecular beam epitaxy (MBE) on a GaAs (100) substrate. First, we grow a 1- μm layer of ZnSe buffer, then two monolayers of (Cd,Mn)Se, which are immediately transformed into QDs, and finally 100 nm of ZnSe cap. The molecular flux of Mn is optimized to assure the high probability of finding QDs with exactly one Mn^{2+} ion in each dot.

For the optical experiments, the sample is placed inside a cryostat equipped with a superconducting magnet producing field up to 10 T in Faraday configuration. The QDs are excited nonresonantly by a continuous-wave (CW) Ar-ion laser at 488.0 nm ($\simeq 2.55$ eV). A reflection microscope objective, immersed in a superfluid He together with the sample (at $T = 1.8$ K), provides a spatial limitation of the photoluminescence (PL) excitation and detection to an area of diameter smaller than 1 μm . Well-separated emission lines of individual QDs are observed in a long-wavelength tail of the PL band.

An example PL spectrum of a QD containing single Mn^{2+} ion is presented in Fig. 1(a). It consists of three groups of emission lines, which originate from the recombination of a neutral exciton (X), negatively charged exciton (X^-), and biexciton ($2X$). This attribution is based on relative emission energies, which match the well-established pattern previously obtained for nonmagnetic CdSe QDs [4,26,27]. The identification of the X^- transition is further confirmed by our observation of negative optical polarization transfer, as was previously done for different QD systems, both III-V [28,29] and II-VI [21,30]. Each of the observed transitions exhibits multifold splitting related to the presence of the $s, p-d$ exchange interaction between confined carriers and Mn^{2+} ion (total spin $S = 5/2$) [4,13,31–34]. In particular, the X emission line is split into six components. Each of them, when detected

*tomasz.smolenski@fuw.edu.pl

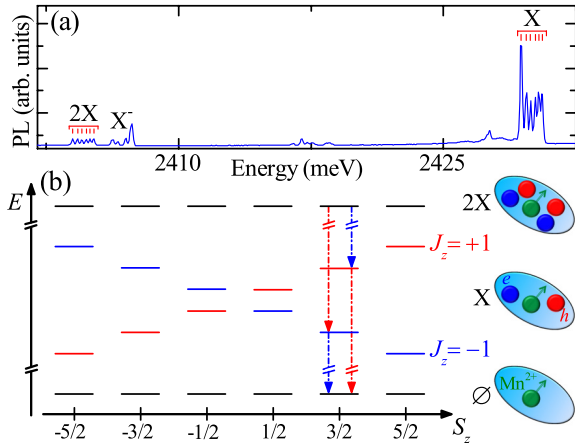


FIG. 1. (Color online) (a) A PL spectrum of a CdSe/ZnSe QD containing a single Mn^{2+} ion. (b) Simplified diagram of neutral exciton and biexciton energy levels in Mn-doped QD at zero magnetic field. The states are displayed as a function of their energy and Mn^{2+} ion spin projection on the QD growth axis. Color of the neutral exciton levels denotes the X spin projection on the growth axis as well as the circular polarization of corresponding X optical transitions (red – σ^+ , blue – σ^-). For clarity, only the transitions related to $3/2$ spin projection of the Mn^{2+} ion are shown.

in a given circular polarization (i.e., for the given exciton spin projection J_z), corresponds to one of six possible Mn^{2+} spin projections S_z on the growth axis [as is schematically shown in Fig. 1(b)]. Similar sixfold splitting is also observed for the spin-singlet biexciton PL spectrum. In that case the splitting is solely related to the final state of the recombination (i.e., the X state), whereas the $2X$ itself does not interact with the ion [see Fig. 1(b)].

III. EXCITON SPIN-TRANSFER

The efficient exciton spin-transfer for a QD with a single Mn^{2+} ion is demonstrated by polarization-resolved measurements of X PL under below-the-barrier CW excitation at 488 nm in the external magnetic field. The results obtained for an example QD are presented in Figs. 2(a) to 2(i). Under circularly polarized excitation we observe a pronounced spin-transfer in the entire range of the applied field, as the copolarized integrated intensities of X PL are clearly larger than the cross-polarized intensities [Figs. 2(a), 2(b), 2(d), 2(e), 2(g), and 2(h)].

The quantitative determination of the spin-polarization degree of injected excitons requires taking into account the possible spin relaxation of the X -Mn system occurring during the X lifetime in a QD. The presence of such relaxation is revealed by the zero-field X PL spectra measured under linearly polarized excitation [Fig. 2(c)]. In such a case, we expect no spin-polarization of the Mn^{2+} ion, which should lead to equal intensities of six emission lines corresponding to different projections of the ion spin. However, the intensity of the low-energy emission line is significantly larger compared to the other lines, independently of the circular polarization of detection. Since the low-energy line corresponds to $\pm 5/2$ ion spin projection in σ^\mp polarization of detection, this effect cannot be attributed to a steady-state polarization of

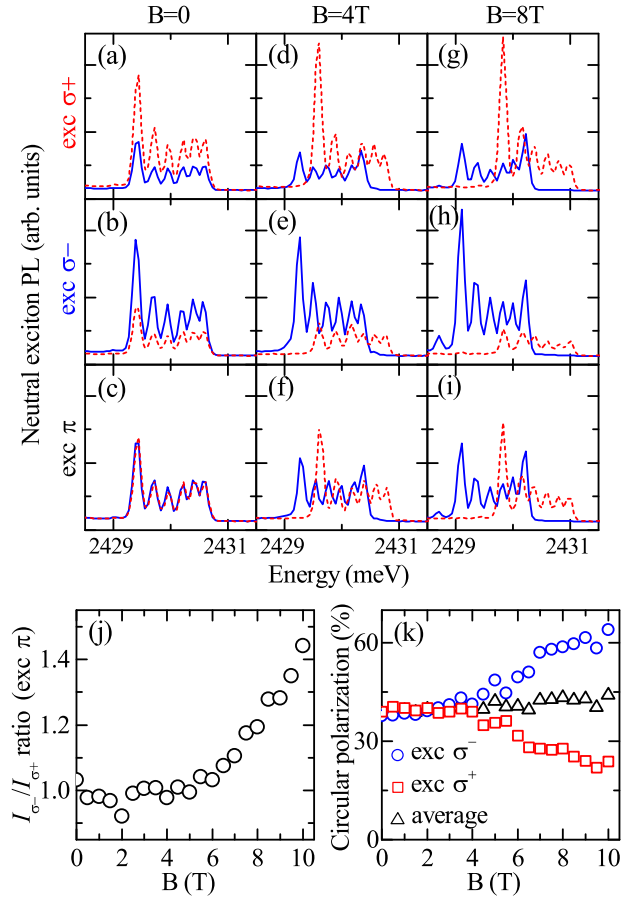


FIG. 2. (Color online) (a)–(i) PL spectra of the neutral exciton confined in Mn-doped QD under excitation at 488 nm with indicated circular or linear polarizations. The spectra were detected in σ^+ (dashed red lines) and σ^- (solid blue lines) circular polarizations and measured at magnetic field (a)–(c) $B = 0$, (d)–(f) $B = 4$ T, and (g)–(i) $B = 8$ T. (j) Magnetic field dependence of the ratio of integrated X PL intensities detected in σ^- and σ^+ circular polarizations under linearly polarized excitation. (k) Circular polarization degree (absolute value) of the integrated X PL under excitation with σ^+ (squares) and σ^- (circles) polarization as a function of the magnetic field. The average values of these two degrees are marked with triangles.

the ion spin. On the other hand, it may originate from the X spin-flip process causing the exciton relaxation from the $|J_z = \pm 1, S_z = \pm 5/2\rangle$ state towards $|J_z = \mp 1, S_z = \pm 5/2\rangle$. As this process does not affect the ion spin, its underlying mechanism is identical to the one entailing exciton spin-flip in a nonmagnetic QD between Zeeman-split states. The latter process is found to be quite efficient in the case of undoped dots in our sample, which suggests that the proposed spin relaxation can also play a significant role in Mn-doped QD. In particular, it increases the intensity of the low-energy X emission line. On the other hand, such a process would also lead to a decrease of the high-energy line intensity, which is, however, not reflected by the experimental results [Fig. 2(c)]. Thus, we expect that additional X -Mn spin relaxation processes have to be also important. They might be related to a mutual flip of exciton and ion spins or a spin-flip of a single carrier forming the neutral exciton resulting in a creation of a dark exciton [35].

The precise identification and detailed description of these relaxation processes remain beyond the scope of this paper and require further study.

The application of the magnetic field lifts the symmetry between energy levels corresponding to $J_z = \pm 1$ excitons. As a consequence, the X-Mn spin relaxation entails a difference of X PL intensities measured in two circular polarizations of detection under linearly polarized excitation [Figs. 2(f) and 2(i)]. As the relative energy of $J_z = -1$ exciton is decreased, the spin-flip processes increase the intensity of the corresponding σ^- polarized X PL. It is clearly visible in Fig. 2(j) presenting the ratio of integrated X PL intensities detected in σ^- and σ^+ polarizations under linearly polarized excitation. The influence of the spin-flip is also visible in the X PL spectra measured under circularly polarized excitation. In such a case, the spin relaxation results in an increase (decrease) of the circular polarization degree of integrated X PL under excitation with σ^- (σ^+) polarization at high magnetic field [Fig. 2(k)]. Therefore, the obtained degrees do not exactly correspond to the spin-polarization degrees of excitons injected to the dot. However, the average degree of circular polarization of X PL under σ^- and σ^+ polarized excitation of about 40% [Fig. 2(k)] defines the lower limit of the exciton spin-transfer efficiency in the entire range of the applied magnetic field.

IV. OPTICAL ORIENTATION OF Mn²⁺ SPIN

Exploiting the ability to inject the spin-polarized excitons to Mn-doped CdSe/ZnSe QD we study their influence on the Mn²⁺ ion spin state. Such an influence so far has been demonstrated for CdTe/ZnTe QDs, in which the single Mn²⁺ ion spin could be oriented towards the $\pm 5/2$ state via its exchange interaction with $J_z = \mp 1$ excitons [18–20]. To examine the presence of this phenomenon in the case of CdSe QDs, we first need to establish a method enabling unambiguous optical readout of the ion spin state. In contrast to the previous studies of CdTe QDs, the Mn²⁺ spin state cannot be determined based on the intensities of six X emission lines due to efficient X-Mn spin relaxation. For this reason we monitor the ion spin based on the intensities of the biexciton emission lines. Since the 2X is a spin singlet, it is decoupled from the ion and its optical transitions act as an almost ideal probe of the ion spin state in an empty dot. A small interaction between the 2X and the Mn²⁺ ion related to a configuration mixing [36] might be neglected here.

The possibility of optical manipulation of the Mn²⁺ ion spin in a CdSe QD is verified by measurements of the biexciton PL spectra performed under circularly or linearly polarized excitation in a fixed circular polarization of detection. This ensures that each 2X emission line corresponds to a specified spin projection of the Mn²⁺ ion. The zero-field spectra detected in σ^- polarization are shown in Figs. 3(a) to 3(c). In the case of linearly polarized excitation, the intensities of all 2X emission lines are almost equal [Fig. 3(a)], which is a direct fingerprint of depolarized ion spin. On the other hand, excitation with circularly polarized light results in a small, but not negligible nonuniform distribution of the intensities between six lines. In particular, under σ^- polarized excitation the lower-energy lines are more intense compared to the higher-energy ones

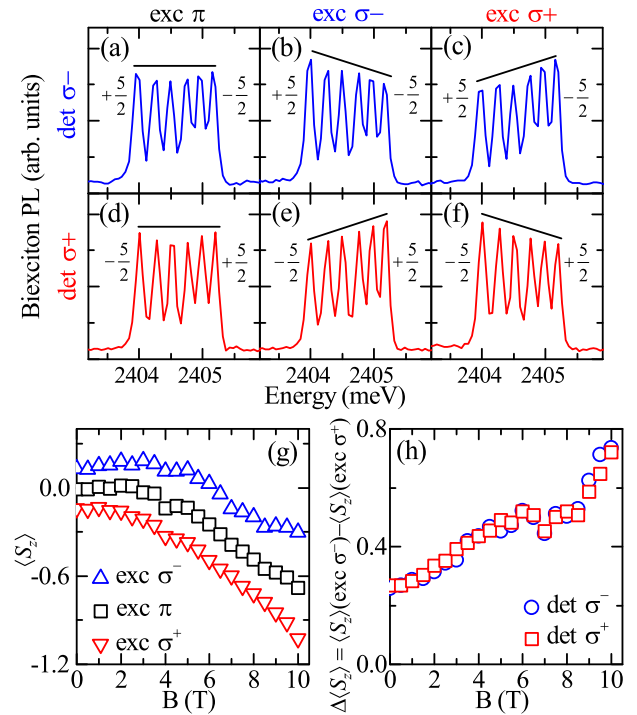


FIG. 3. (Color online) (a)–(f) The zero-field PL spectra of biexciton confined in Mn-doped QD. The spectra were excited with indicated circular or linear polarizations and detected in σ^- [(a)–(c) blue] and σ^+ [(d)–(f) red] polarizations. The ion spin projections corresponding to the emission lines of extreme energies are indicated. Solid lines representing the directions of change of 2X intensities are drawn to guide the eye. (g) Magnetic field dependence of the mean spin of the Mn²⁺ ion determined in σ^+ polarization of detection under linearly or circularly polarized excitation (as indicated). (h) The efficiency of optically induced Mn²⁺ spin orientation measured as a function of the magnetic field. Circles (squares) represent the efficiencies determined in σ^- (σ^+) polarization of detection. The excitation power was kept well below the saturation power.

[Fig. 3(b)]. Switching the polarization of excitation to σ^+ leads to the opposite effect [Fig. 3(c)]. Since σ^- polarized 2X emission lines of subsequent energies correspond to Mn²⁺ spin projections ranging from $5/2$ to $-5/2$, our observations indicate that the injection of $J_z = \pm 1$ excitons orients the ion spin towards the $\mp 5/2$ state, similarly to the case of Mn-doped CdTe QDs [18–20]. The Mn²⁺ spin can be also independently probed in σ^+ polarization of detection [Figs. 3(d) to 3(f)]. In such a case, the 2X emission energies correspond to subsequent ion spin projections in a reversed order, namely ranging from $-5/2$ to $5/2$. As the ion spin state depends only on the spin of injected excitons, we observe the opposite change of intensities of 2X emission lines under the same circular polarization of excitation compared to the previously used σ^- polarization of detection, which is clearly seen in Figs. 3(e) and 3(f).

The ion spin-polarization can be quantitatively measured as the Mn²⁺ mean spin $\langle S_z \rangle$. It is directly determined from the 2X PL spectrum detected in a circular polarization as a weighted average of the intensities of consecutive emission lines. Magnetic field dependencies of $\langle S_z \rangle$ obtained under different polarizations of excitation are shown in Fig. 3(g). In

the case of linearly polarized excitation, a pronounced decrease of $\langle S_z \rangle$ with increasing B directly reflects the thermalization of the ion spin towards the $-5/2$ state arising due to the ion Zeeman splitting. On the other hand, excitation with σ^- (σ^+) polarization increases (decreases) the ion mean spin, which confirms the feasibility of the optical spin orientation in the entire range of the applied field. To perform an analysis of the efficiency of this orientation, we introduce its quantitative measure defined as a difference $\Delta\langle S_z \rangle$ between the ion mean spin determined under σ^- and σ^+ polarized excitation. The dependence of this value on the magnetic field is shown in Fig. 3(h). The presented data are obtained under sufficiently low excitation power assuring that both the optically induced exciton spin-transfer and the ion spin orientation are not affected by an excess of created biexcitons [19]. Since the mean spin of the Mn^{2+} ion can be independently measured based on the spectra detected in two circular polarizations, Fig. 3(h) contains two sets of points corresponding to σ^+ and σ^- polarized detections. Their mutual agreement confirms the self-consistency of our experimental results.

The determined spin orientation efficiency clearly increases with the magnetic field (from $\Delta\langle S_z \rangle/2S \approx 5\%$ at zero field to about 15% at $B = 10$ T). In the low-field regime, such an effect can be attributed to a suppression of the mixing between Mn^{2+} spin eigenstates introduced by a hyperfine interaction with nuclear spin. This mixing was previously shown to significantly increase the ion spin relaxation dynamics in the absence of the magnetic field [19,37–39], which finally decreases the zero-field efficiency of optical pumping of the ion spin. However, the hyperfine coupling is relatively small [40] and even a field of the order of few tenths of Tesla is sufficient to almost completely purify the ion spin eigenstates. As a result, it cannot be the underlying reason of the pronounced enhancement of spin orientation efficiency at $B > 1$ T. Taking into account the almost constant exciton spin-transfer efficiency in the entire range of the applied field, this enhancement reflects the field dependence of the intrinsic mechanism leading to the ion spin orientation. Surprisingly, no theoretical model providing such a mechanism has been proposed so far, despite the intuitive character of the optical orientation process. In particular, only the optical pumping of the ion spin under strictly resonant excitation [15,16] was quantitatively understood [35,41].

V. CONCLUSION

We have demonstrated the optical spin orientation of a single Mn^{2+} ion embedded in a CdSe/ZnSe QD. It was achieved through the injection of spin-polarized excitons to the dot under circularly polarized excitation at 488 nm, which provided high spin-transfer efficiency of about 40% in the entire range of the applied magnetic field (0–10 T). The ion spin readout was based on the intensities of six $2X$ emission lines detected in a circular polarization. Our findings revealed that under σ^\pm polarized excitation the Mn^{2+} spin is oriented towards the $\mp 5/2$ state. The efficiency of the optical orientation was found to increase with the magnetic field (from about 5% at $B = 0$ to 15% at $B = 10$ T). Simultaneously, it was a few times lower compared to the previously studied Mn-doped CdTe QDs [19], for even higher efficiency of the exciton spin-transfer in the present case. This observation together with the indication of several differences between the two types of dots, including much more efficient exciton spin relaxation for CdSe QDs, may shed some light on the mechanism of the ion spin orientation and help in its further investigation. On the other hand, the possibility of the optical control over the Mn^{2+} spin in a CdSe QD evidenced in our work may be further exploited to determine the ion spin relaxation dynamics in a low-field regime or even in the absence of the magnetic field.

ACKNOWLEDGMENTS

The authors thank Tomasz Kazimierzczuk for stimulating discussions. This work was supported by the Polish Ministry of Science and Higher Education in the years 2012–2016 as a research grant “Diamantowy Grant”; by the Polish National Science Centre under Grants No. DEC-2011/01/B/ST3/02406, No. DEC-2011/02/A/ST3/00131, No. DEC-2012/07/N/ST3/03130, No. DEC-2013/09/B/ST3/02603, and No. DEC-2013/09/D/ST3/03768; by the Polish National Centre for Research and Development project LIDER; and by the Foundation for Polish Science (FNP) subsidy “Mistrz.” The project was carried out with the use of CePT, CeZaMat, and NLTK infrastructures financed by the European Union—the European Regional Development Fund within the Operational Programme “Innovative economy” for 2007–2013.

-
- [1] P. M. Koenraad and M. E. Flatté, *Nat. Mater.* **10**, 91 (2011).
 - [2] D. D. Awschalom, L. C. Bassett, A. S. Dzurak, E. L. Hu, and J. R. Petta, *Science* **339**, 1174 (2013).
 - [3] J. Fernández-Rossier, *Nat. Mater.* **12**, 480 (2013).
 - [4] J. Kobak, T. Smoleński, M. Goryca, M. Papaj, K. Gietka, A. Bogucki, M. Koperski, J.-G. Rousset, J. Suffczyński, E. Janik, M. Nawrocki, A. Gólnik, P. Kossacki, and W. Pacuski, *Nat. Commun.* **5**, 3191 (2014).
 - [5] M. Fuechsle, J. A. Miwa, S. Mahapatra, H. Ryu, S. Lee, O. Warschkow, L. C. Hollenberg, G. Klimeck, and M. Y. Simmons, *Nat. Nanotechnol.* **7**, 242 (2012).
 - [6] J. J. Pla, K. Y. Tan, J. P. Dehollain, W. H. Lim, J. J. Morton, D. N. Jamieson, A. S. Dzurak, and A. Morello, *Nature (London)* **489**, 541 (2012).
 - [7] H. Büch, S. Mahapatra, R. Rahman, A. Morello, and M. Y. Simmons, *Nat. Commun.* **4**, 2017 (2013).
 - [8] F. Jelezko, T. Gaebel, I. Popa, A. Gruber, and J. Wrachtrup, *Phys. Rev. Lett.* **92**, 076401 (2004).
 - [9] C. Yin, M. Rancic, G. G. de Boo, N. Stavrias, J. C. McCallum, M. J. Sellars, and S. Rogge, *Nature (London)* **497**, 91 (2013).
 - [10] P. Siyushev, K. Xia, R. Reuter, M. Jamali, N. Zhao, N. Yang, C. Duan, N. Kukharchyk, A. D. Wieck, R. Kolesov, and J. Wrachtrup, *Nat. Commun.* **5**, 3895 (2014).
 - [11] T. Utikal, E. Eichhammer, L. Petersen, A. Renn, S. Götzinger, and V. Sandoghdar, *Nat. Commun.* **5**, 3627 (2014).
 - [12] J. A. Gaj and J. Kossut, in *Introduction to the Physics of Diluted Magnetic Semiconductors*, Springer Series in Materials Science, (Springer, Heidelberg, Germany, 2010), Vol. 144, pp. 1–36.

- [13] L. Besombes, Y. Léger, L. Maingault, D. Ferrand, H. Mariette, and J. Cibert, *Phys. Rev. Lett.* **93**, 207403 (2004).
- [14] A. Kudelski, A. Lemaître, A. Miard, P. Voisin, T. C. M. Graham, R. J. Warburton, and O. Krebs, *Phys. Rev. Lett.* **99**, 247209 (2007).
- [15] C. Le Gall, R. S. Kolodka, C. L. Cao, H. Boukari, H. Mariette, J. Fernández-Rossier, and L. Besombes, *Phys. Rev. B* **81**, 245315 (2010).
- [16] E. Baudin, E. Benjamin, A. Lemaître, and O. Krebs, *Phys. Rev. Lett.* **107**, 197402 (2011).
- [17] M. Goryca, M. Koperski, P. Wojnar, T. Smoleński, T. Kazimierzczuk, A. Golnik, and P. Kossacki, *Phys. Rev. Lett.* **113**, 227202 (2014).
- [18] C. Le Gall, L. Besombes, H. Boukari, R. Kolodka, J. Cibert, and H. Mariette, *Phys. Rev. Lett.* **102**, 127402 (2009).
- [19] M. Goryca, T. Kazimierzczuk, M. Nawrocki, A. Golnik, J. A. Gaj, P. Kossacki, P. Wojnar, and G. Karczewski, *Phys. Rev. Lett.* **103**, 087401 (2009).
- [20] M. Goryca, T. Kazimierzczuk, M. Nawrocki, A. Golnik, J. Gaj, P. Wojnar, G. Karczewski, and P. Kossacki, *Physica E* **42**, 2690 (2010).
- [21] T. Kazimierzczuk, J. Suffczyński, A. Golnik, J. A. Gaj, P. Kossacki, and P. Wojnar, *Phys. Rev. B* **79**, 153301 (2009).
- [22] M. Koperski, M. Goryca, T. Kazimierzczuk, T. Smoleński, A. Golnik, P. Wojnar, and P. Kossacki, *Phys. Rev. B* **89**, 075311 (2014).
- [23] T. Smoleński, [arXiv:1408.1981](https://arxiv.org/abs/1408.1981).
- [24] M. Pilat, M. Goryca, T. Smoleński, W. Pacuski, and P. Kossacki, *Acta Phys. Pol. A* **126**, 1212 (2014).
- [25] Y. G. Kusrayev, A. V. Koudinov, B. P. Zakharchenya, S. Lee, J. K. Furdyna, and M. Dobrowolska, *Phys. Rev. B* **72**, 155301 (2005).
- [26] B. Patton, W. Langbein, and U. Woggon, *Phys. Rev. B* **68**, 125316 (2003).
- [27] M. Koch, K. Kheng, I. C. Robin, and R. André, *Phys. Status Solidi C* **3**, 3916 (2006).
- [28] S. Cortez, O. Krebs, S. Laurent, M. Senes, X. Marie, P. Voisin, R. Ferreira, G. Bastard, J.-M. Gérard, and T. Amand, *Phys. Rev. Lett.* **89**, 207401 (2002).
- [29] S. Laurent, M. Senes, O. Krebs, V. K. Kalevich, B. Urbaszek, X. Marie, T. Amand, and P. Voisin, *Phys. Rev. B* **73**, 235302 (2006).
- [30] I. A. Akimov, D. H. Feng, and F. Henneberger, *Phys. Rev. Lett.* **97**, 056602 (2006).
- [31] Y. Léger, L. Besombes, L. Maingault, D. Ferrand, and H. Mariette, *Phys. Rev. Lett.* **95**, 047403 (2005).
- [32] Y. Léger, L. Besombes, J. Fernández-Rossier, L. Maingault, and H. Mariette, *Phys. Rev. Lett.* **97**, 107401 (2006).
- [33] Y. Léger, L. Besombes, L. Maingault, and H. Mariette, *Phys. Rev. B* **76**, 045331 (2007).
- [34] M. Goryca, P. Plochocka, T. Kazimierzczuk, P. Wojnar, G. Karczewski, J. A. Gaj, M. Potemski, and P. Kossacki, *Phys. Rev. B* **82**, 165323 (2010).
- [35] L. Cywiński, *Phys. Rev. B* **82**, 075321 (2010).
- [36] A. H. Trojnar, M. Korkusinski, U. C. Mendes, M. Goryca, M. Koperski, T. Smolenski, P. Kossacki, P. Wojnar, and P. Hawrylak, *Phys. Rev. B* **87**, 205311 (2013).
- [37] M. Goryca, D. Ferrand, P. Kossacki, M. Nawrocki, W. Pacuski, W. Maślana, J. A. Gaj, S. Tatarenko, J. Cibert, T. Wojtowicz, and G. Karczewski, *Phys. Rev. Lett.* **102**, 046408 (2009).
- [38] P. Kossacki, D. Ferrand, M. Goryca, M. Nawrocki, W. Pacuski, W. Maślana, S. Tatarenko, and J. Cibert, *Physica E* **32**, 454 (2006).
- [39] M. Goryca, D. Ferrand, P. Kossacki, M. Nawrocki, W. Pacuski, W. Maślana, S. Tatarenko, and J. Cibert, *Phys. Status Solidi B* **243**, 882 (2006).
- [40] M. Quazzaz, G. Yang, S. Xin, L. Montes, H. Luo, and J. K. Furdyna, *Solid State Commun.* **96**, 405 (1995).
- [41] C. L. Cao, L. Besombes, and J. Fernández-Rossier, *Phys. Rev. B* **84**, 205305 (2011).